Designing Organic/Inorganic Colloids by Heterophase Polymerization

Elodie Bourgeat-Lami,[*1] *Norma Negrete Herrera,*[1] *Jean-Luc Putaux,*[2] *Adeline Perro,*[3] *Stéphane Reculusa,*[3] *Serge Ravaine,*[3] *Etienne Duguet*[4]

Summary: Polymer/silica and polymer/Laponite nanocomposite colloids with various morphologies have been elaborated through emulsion polymerization using a polymerizable organosilane (route I) and a methyl methacrylate-terminated macromonomer (route II) as coupling agents. Depending on the synthetic strategy and on the nature of the mineral particles, either core-shell, raspberry-like, multipod-like, currant bun or inverted core-shell morphologies (the mineral forming the shell) were achieved. Beyond the control of particle shape, we have demonstrated that some of the polymerizations exhibited particular kinetics behaviors which could be correlated to the mechanism of formation of the composite particles. Interestingly, conversion versus time curves of a series of soap free polymerizations performed in the presence of the macromonomer showed a significant increase in the polymerization rate with increasing the inorganic particles concentration. Characterization of the composite latexes by transmission electron microscopy showed that the mineral was located at the surface of the latex spheres and participated therefore to their stabilization. The higher the amount of inorganic particles, the lower the particles size and the higher the polymerization rate.

Keywords: emulsion polymerization; kinetics; laponite; nanocomposite colloids; silica

Introduction

The combination of organic and inorganic components into composite colloids is attracting increasing interest as it enables to create new nanostructured materials with unsual shapes, compositions and properties originating from their starting components.[1–6] Among the various techniques, *in situ* polymerization offers many advantages compared to physical approaches as it allows controlling the nature and the chemical composition of the polymer. *In situ* polymerization generally involves polymerizing in the presence of mineral particles which have been previously functionalized in order to promote polymer chain growth on their surface.[1] Once performed in dispersed media, this strategy allows designing organic/inorganic colloids with completely original shapes and morphologies (core-shell, multicores, raspberry-like, dumbell-like, currant bun, etc.) which cannot be achieved by simply mixing organic and inorganic particles. These colloids can additionnaly be used as building blocks to fabricate nano or microstructured materials with tailored textural, optical or mechanical properties. During the last ten years, we and others have developped various routes to such nanostructured colloids by heterophase polymerization including suspension,[7] dispersion,[8,9] miniemulsion[10–12] and emulsion polymerizations.[13–27] Although there have

[1] Laboratoire de Chimie et Procédés de Polymérisation - CNRS-CPE Lyon - Bâtiment 308 F, 43, boulevard du 11 novembre 1918 - BP 2077 - 69616 Villeurbanne Cedex, France
[2] Centre de Recherches sur les Macromolécules Végétales, ICMG/CNRS, BP 53, F-38041 Grenoble Cedex 9, France
[3] Centre de Recherche Paul Pascal – CNRS, 115, avenue du Dr Schweitzer - 33600 Pessac, France
[4] Institut de Chimie de la Matière Condensée de Bordeaux – CNRS - 87, avenue du Dr Schweitzer - 33608 Pessac Cedex, France

been immense efforts to synthesise well defined organic/inorganic particles in multiphase media, much less attention has been paid to the mechanistic aspects of the polymerization reaction in such complex systems. In this article, we report recent results along this line on the elaboration of organic/inorganic colloids through emulsion polymerization following two routes. In a first method, organic modification of the mineral particles was performed by grafting organosilane molecules bearing a reactive methacrylate functionality (Structures 1 and 2) while in the second method, the organic modification was performed by adsorption of a methyl methacrylate-terminated polyethylene glycol macromonomer (PEG-MA, Structure 3). The article is divided in two parts. The first part is devoted to the synthesis of silica/polystyrene composite particles while the second part reports the elaboration of clay-based composite particles using organically-modified anisotropic Laponite platelets as seeds. The paper describes the surface modification of the mineral particles and addresses the effect of the experimental parameters on the composite particles morphology, polymerization kinetics and mechanism.

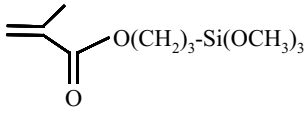

Structure 1 : MPS

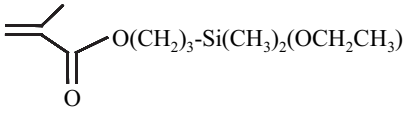

Structure 2 : MPDES

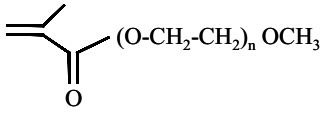

Structure 3 : PEG-MA

Experimental Part

Materials

Commercial silica sols with diameters of 13 and 80 nm and a solid content of around 30% (Klebosol 30N12 and Klebosol 30N50, respectively) were kindly supplied by Clariant. The 30N50 silica sol was used as received meanwhile 30N12 was dialyzed against desionized water until the obtention of a neutral *pH* before use. Suspensions of silica particles in a mixture of ethanol and water, with diameters of 500 nm and 1 μm, respectively, were prepared according to the procedure of Stöber et al. as described previously.[21] They were evaporated in order to remove part of ammonia and ethanol and to reduce the volume of the suspension. The latter was then dialyzed against water until *pH* 7. Its final concentration was determined gravimetrically and adjusted to the desired value before use. Laponite RD with a cation exchange capacity of 0.75 $meq \cdot g^{-1}$ was supplied from Laporte Industries and used without further purification.

γ-Methacryloyloxypropyl trimethoxysilane (MPS, $M_w = 248.3\ g \cdot mol^{-1}$, Aldrich), and γ-methacryloyloxypropyl dimethylethoxysilane (MPDES, $M_w = 230.3\ g \cdot mol^{-1}$, Gelest), were used as supplied. The macromonomer, poly(ethylene glycol) 1000 monomethylether methacrylate (PEG-MA) was obtained from Polysciences. The peptizing agent: tetrasodium pyrophosphate ($Na_4P_2O_7$, Aldrich), the monomers: styrene (Sty, Aldrich), methyl methacrylate (MMA, Aldrich) and butyl acrylate (BuA, Aldrich) and the initiators: potassium persulfate (KPS, Acros Organics) and azo-bis cyano pentanoic acid (ACPA, Wako Chemicals) were used as received. The anionic surfactant, sodium dodecyl sulfate (SDS, $M_w = 288.4\ g \cdot mol^{-1}$, Acros Organics) and the nonylphenol poly(oxyethylenic) nonionic surfactant (Remcopal NP_{30}, $M_w = 1540\ g \cdot mol^{-1}$, a gift from CECA S.A, Paris), were of analytical grade and used as supplied. Deionized water was purified by a Milli-Q Academic system (Millipore Cooperation).

Organic Modification Procedures

Silica

Grafting of the commercial Klebosol 30N50 silica sol was performed by introducing known amounts of MPS into 100 mL of a 10 $g \cdot L^{-1}$ stock silica suspension containing 1 $g \cdot L^{-1}$ of SDS. The dispersions were stirred magnetically at ambient temperature and allowed to equilibrate for 19 hours. They were next centrifuged and the supernatant solutions were analyzed by UV spectroscopy. The amount of grafted MPS, Q_{MPS} ($\mu mol \cdot m^{-2}$), was determined by difference between the total amount and the free amount of MPS using a predetermined calibration curve established on silica-free suspensions of identical composition as reported elsewhere.[23] Macromonomer adsorption was performed by adding a known amount of a calibrated PEG-methacrylate solution to a known amount of the aqueous silica suspension in a capped glass vessel. The dispersion was shaken magnetically at ambient temperature and allowed to equilibrate for 24 hours.

Laponite

Grafting of the MPS and MPDES molecules on the Laponite clay edges was performed as follows. 1 g of Laponite was suspended into 100 mL of toluene and a known amount of the coupling agent (comprised between 0.75 and 7 mmoles) was introduced in the reaction flask and allowed to react for 21 days at room temperature. The grafted Laponites were filtered, extensively washed with toluene in order to remove the excess of functional alkoxysilane, and dried overnight in a vacuum oven at 40 °C before characterization. The grafted amount, expressed in mmoles of grafted silane per g of bare laponite, was determined from the difference ΔC(wt%) of carbon content after and before grafting as described elsewhere.[28]

Emulsion Polymerization

Silica/Polystyrene Nanocomposite Particles

The polymerization reactions were carried out in batch at 70 °C for up to 24 hours under nitrogen atmosphere. The 300 mL glass reactor fitted with a condenser was charged with the organically-modified silica suspension and the surfactant. Degassing was carried out for 30 minutes under gentle stirring before increasing the temperature up to 70 °C. Then, the required amounts of KPS, dissolved in 10 mL of de-ionized water, and of monomer were added at once to start polymerization. A typical recipe involving MPS as coupling agent is as follows: MPS-functionalized silica, 1 g; water, 100 g; styrene, 10 g; KPS, 0.1 g and SDS, 0.1 g · Polymerizations performed in the presence of PEG-MA were conducted as follows. Typically, the silica suspension (10 $g \cdot L^{-1}$) containing predetermined amounts of macromonomer (1.5$\mu mol/m^2$ silica) and surfactant (NP_{30}, 3 $g \cdot L^{-1}$) was charged into the reactor. After degassing at 70 °C, the monomer (styrene, 100 $g \cdot L^{-1}$) was introduced at once under stirring followed by the initiator (KPS, 1 $g \cdot L^{-1}$). A series of soap-free emulsion polymerizations of styrene and MMA were performed in the presence of the Klebosol 30N12 silica as follows. A known quantity of the macromonomer (2.5 wt%, respect to silica) was introduced into the silica suspension (concentration comprised between 10 and 80 $g \cdot L^{-1}$) and the mixture was allowed to equilibrate for one night. The suspension was next introduced into the reactor and purged with nitrogen at 70 °C. Then, after degassing, the monomers (styrene: 160 $g \cdot L^{-1}$ and MMA: 40 $g \cdot L^{-1}$) were added at once under strong agitation and the polymerization was initiated by the addition of the initiator (KPS, 1 $g \cdot L^{-1}$).

Clay-based Nanocomposite Particles

Emulsion polymerization was carried out at 70 °C in a 250 mL three-necked double wall reactor equipped with a condenser, a nitrogen inlet tube and a stirrer. A typical recipe for MPDES-grafted Laponites is as follows. The reactor was charged with 100 g of the aqueous MPDES-grafted Laponite suspension (10 $g \cdot L^{-1}$) containing the surfactant (SDS, 2 $g \cdot L^{-1}$) and the peptizing agent ($Na_4P_2O_7$, 1 $g \cdot L^{-1}$). After degassing,

the monomers, a mixture of styrene (3 g) and butyl acrylate (7 g), and the initiator (ACPA, 0.1 g) were successively introduced at 70 °C under stirring. Polymerizations performed using the PEG-MA/clay complexes involved slighlty different experimental conditions. In a typical run, Laponite (3 g) was first suspended in water (150 g) and magnetically stirred for 1 h to totally exfoliate the clay tactoïds. Then, the macromonomer (0.15 g) and the peptizing agent (0.3 g) were introduced in the clay suspension and the mixture was fed to the reactor followed by the monomer (styrene, 30 g). The polymerization was initiated by introducing 0.15 g of ACPA dissolved into 3 mL of water.

Characterizations

UV analysis was performed using an UV/VIS spectrophotometer and quartz cells. The measurements were carried out at the wavelength of 205 nm. A JEOL JCXA 733 electron microprobe analyzer was used to determine the carbon content of the bare and organically-modified Laponite samples. The monomer-to-polymer conversions were determined gravimetrically. Typically, 3–7 g of the latex suspension was placed in an aluminium dish and dried to constant weight at 70 °C. Particle size was determined by dynamic light scattering (DLS). The morphology of the nanocomposite particles was characterized by ''conventional'' transmission electron microscopy (TEM) and cryogenic transmission electron microscopy (cryo-TEM). Specimens for TEM were prepared by evaporating one drop of dilute latex (10^{-3}/10^{-6} $g \cdot cm^{-3}$) on a 200 mesh formvar-coated copper electron microscope grid. The grids were placed in the vacuum chamber of a Philips CM120 electron microscope operating at 80 kV and observed under low illumination dose. The diameters of the polymer particles were measured directly from the electron micrographs. A minimum of 100 particles were counted for each batch. The number average diameter, D_n, was calculated using Equation 1 where *ni* designates the number of particles of diameter *Di*.

$$Dn = \frac{\sum niDi}{\sum ni} \quad (1)$$

The weight average diameter, D_w, was calculated from:

$$Dw = \frac{\sum niD_i^4}{\sum niD_i^3} \quad (2)$$

and the polydispersity index (*PDI*) was given by:

$$PDI = \frac{Dw}{Dn} \quad (3)$$

Following procedures described elsewhere,[9,29,30] specimens for cryo-TEM analysis were prepared by quench-freezing thin films of the latex suspensions in liquid ethane. They were then mounted in a Gatan 626 cryo-holder, transferred in a Philips CM200 'Cryo' electron microscope operating at 80 kV, and observed at low temperature (−180 °C) under low dose illumination. Images were recorded on Kodak SO163 films. The particle number per unit volume of water (*Np/L*) was calculated by the following equation:

$$Np/L = \frac{\frac{M}{\rho}}{\frac{\pi}{6}Dn^3 \cdot V} \times 10^{19} \quad (4)$$

where *M* (g) is the total mass of solid, ρ ($g \cdot cm^{-3}$) is the density of the particles, *Dn* (nm) is the number average particles diameter determined either from the TEM micrographs or by DLS, and *V* (in liter) is the total volume of water.

Results and Discussion

Silica/Polystyrene Composite Particles

Grafting of γ-methacryloyloxypropyl trimethoxysilane

The grafting was carried out at $pH = 9.5$ by direct addition of MPS to the aqueous colloidal suspension of the Klebosol 30N50 silica particles containing 1 $g \cdot L^{-1}$ of the anionic SDS surfactant. The role of the surfactant is to help disperse the MPS

molecules in water and achieve high grafting densities. Controlling the MPS grafting density is essential as the growing polystyryl radicals are expected to copolymerize with the double bonds of silica, and thus promote the formation of composite particles. The amount of chemisorbed MPS was determined by UV titration of the supernatant solutions recovered by centrifugation of the suspension medium according to the so-called depletion method. This method allowed accurate determination of the MPS grafting density even for low initial concentrations. The MPS grafting densities are indicated in Table 1 as a function of the MPS concentration. The higher the silane concentration, the higher the MPS grafting density in agreement with previous works reported in the literature for related systems.[31]

In order to investigate the effect of the amount of double bonds on the composite particles morphology, a series of polymerization experiments were performed in the presence of the MPS-grafted silica suspensions under otherwise identical conditions in order to analyse the effect of the MPS grafting density only. Figure 1 shows the TEM images obtained for grafting densities of 0,0.95 and 1.9 $\mu mol \cdot m^{-2}$, respectively. For the sake of clarity, micrographs were recorded at low and high magnification to better visualize the particles shape. It can be seen from Figure 1 that the polymerization performed in the presence of non-grafted silica particles gave rise to separate populations of silica beads and polymer latexes with no apparent interaction between them. For all the other experiments, the latex spheres showed more or less affinity for the silica surface indicating that the organic modification is essential in order to yield nanocomposite particle morphologies. For very low MPS grafting densities (typically below $0.5 \mu mole \cdot m^{-2}$), irregular daisy-shaped morphologies were produced with only a few colloids surrounding the silica spheres in an irregular fashion. When the MPS grafting density increases and reaches a value close to e.g., $1 \mu mole \cdot m^{-2}$, most of the polymer latexes are located around the silica particles in more regular flower-like morphologies, each particle being surrounded in average by eight polystyrene petals, as determined by the ratio of the number of polymer particles to the number of silica particles. With increasing further the MPS grafting density, core-shell particles were obtained as shown in Figure 1c. It is also noticeable on these TEM pictures that the diameter of the polystyrene particles is not constant in the different experiments, and hence is the overall particle number and overall surface area.

Table 1 summarizes the particle size and size distribution of the polystyrene latexes directly determined from the TEM micrographs as a function of the MPS grafting density. It can be seen that the number of polystyrene latex particles increases with increasing the MPS grafting density and then decreases for larger MPS concentrations to reach a value which is identical to that determined in the absence of silica particles. This result suggests that for low

Table 1.
Number average particle diameters, weight average particle diameters and polydispersity indexes of polystyrene latex particles synthesized in the presence of MPS-grafted 30N50 silica particles with increasing MPS grafting densities.

[MPS] ($\mu mol \cdot m^{-2}$)	Q_{MPS} ($\mu mol \cdot m^{-2}$)	Conversion (%)	D_n (nm)	D_w (nm)	D_w/D_n	Np/L
0	0	100	197.2	201.1	1.02	$2.5\ 10^{16}$
0.1	0.1	96	129.5	143.4	1.11	$8.4\ 10^{16}$
0.2	0.2	95	113.9	128.3	1.13	$1.2\ 10^{17}$
0.5	0.35	86	92.8	113.6	1.22	$2.1\ 10^{17}$
1	0.65	96.2	110.5	122.6	1.11	$1.4\ 10^{17}$
2	0.95	99.6	113.0	116.9	1.03	$1.3\ 10^{17}$
10	1.9	98.5	190.5	194.3	1.02	$2.5\ 10^{16}$

$[SiO_2] = 10\ g \cdot L^{-1}$, $[SDS] = 1\ g \cdot L^{-1}$, [Styrene] = $100\ g \cdot L^{-1}$, KPS = 0.5 wt% relative to styrene.

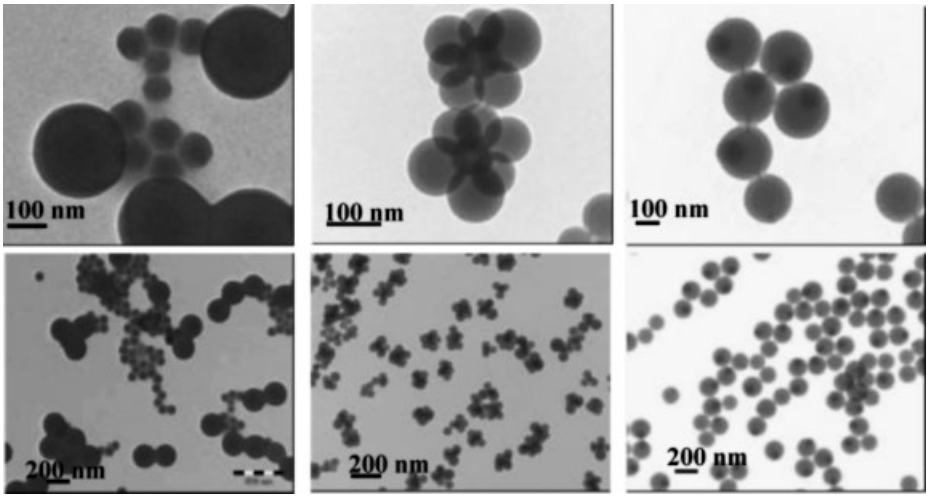

Figure 1.
TEM images of Klebosol 30N50 silica/polystyrene composite particles obtained for different MPS grafting densities. (a) without MPS, (b) $Q_{MPS} = 0.95\ \mu mol \cdot m^{-2}$, and (c) $Q_{MPS} = 1.9\ \mu mol \cdot m^{-2}$. The images were recorded at low (bottom) and high magnifications (top).

MPS grafting densities, the silica particles are able to stabilize the growing polymer spheres and generate a greater latex particle number than when SDS is used as surfactant alone. This is presumably due to the presence of negative charges on the silica surface that enable electrostatic stabilization of the growing polystyrene nodules. However, when the MPS grafting density increases, the polymer spheres no longer phase-segregate on the silica surface and the diameter of the resulting core-shell composite particles increases to reach the value corresponding to pure polymer particles stabilized by surfactant only. As it is known that the rate in emulsion polymerization is proportional to the particle number, one can expect the polymerization kinetics to be influenced by the MPS grafting density (which in turn leads to different polystyrene particles size). The results shown in Figure 2 indicate that, as predicted, the polymerization rate increases with increasing the MPS grafting density and then decreases in agreement with the particles size evolution.

The mechanism of formation of the silica/polystyrene composite particles using MPS as coupling agent can be explained as follows. First, persulfate initiator starts to decompose in the water phase giving rise to the formation of radicals. These radicals will propagate with aqueous phase monomers until they undergo one of the following fates: i) aqueous phase termination or ii) entry into a micelle or precipitation (depending on the surfactant concentration), creating somehow a new particle. Aqueous-phase oligomers of all degree of polymerization can also undergo frequent collision with the surface of the silica seed particles, and have therefore a high probability to copolymerize with the double bonds at the silica surface, thus generating chemisorbed polymer chains in the early stages of polymerization. These discrete loci of adsorption are preferred to adsorb monomer or radicals compared with the bare seed surface. As a result, these discrete loci of adsorption become discrete loci of polymerization. The higher the MPS grafting density, the higher the probability of free radicals capture by silica and therefore the higher the affinity of the growing polymer for the surface. The nucleated polystyrene nodules can thus coalesce and

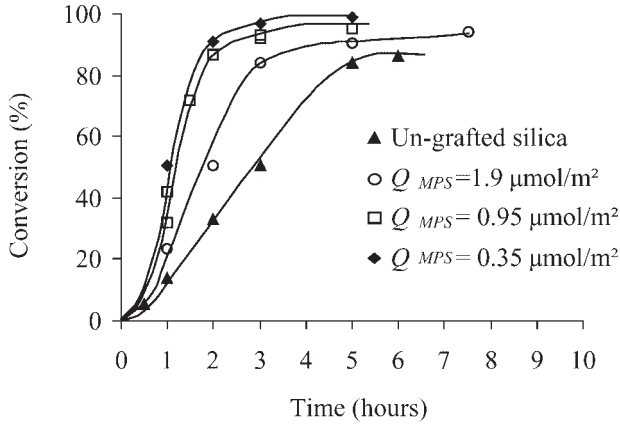

Figure 2.
Conversion versus time curves for polymerization of styrene performed in the presence of Klebosol 30N50 silica particles with increasing amounts of MPS on their surface. Q_{MPS} indicates the actual MPS grafting density as determined by UV analysis using the depletion method.

form a homogeneous coating around the silica seed particles with no change in the overall surface area (i.e., the particles number is kept constant) whereas for low MPS grafting densities, the hydrophilic nature of the surface promotes phase segregation of the growing polymer spheres, the later being presumably stabilized by the negative charges of silica together with adsorbed surfactant molecules. Therefore, the number of polymer particles increased by one order of magnitude which had a significant influence on the polymerization kinetics as shown above.

Adsorption of a Polyethylene Glycol-based Macromonomer

Apart from the use of a polymerizable alkoxysilane, silica/polystyrene composite particles with a raspberry-like morphology have been elaborated in the presence of a methyl methacrylate-terminated polyethylene glycol macromonomer. This macromonomer is mainly hydrophilic due to the presence of ethylene oxide repeat units ($n \sim 23$), which are able to form hydrogen bonds with the silanol groups of silica and adsorb on its surface.[32] In addition, this molecule contains a methacrylate functionality able to copolymerize with styrene thus promoting *in situ* formation of composite particles. As a part of this work, we indeed demonstrated that polymerizations performed in the absence of the macromonomer did not give rise to composite colloids and produced instead separate populations of silica beads and latex spheres. In contrast, when the polymerization was carried out in the presence of micron-size silica beads and a tinny amount of the macromonomer ($1.5\mu mol/m^2$ of silica), hybrid particles with a raspberry-like morphology were successfully obtained (Figure 3). It must be mentioned that free polymer spheres were also present at the end of polymerization but due to the large difference between silica and polystyrene densities, they could be separated from the composite particles by centrifugation which enabled us to observe the morphology of the hybrid particles alone. To investigate the effect of the silica particles size on particles morphology, we synthesized silica spheres of various diameters using a procedure inspired from the literature[33,34] and compared them to very small silica particles of commercial origin. Figure 3 shows the TEM micrographs of the resulting composite particles obtained for silica particles with diameters of 1000, 500 and 13 nm, respectively. In these pictures,

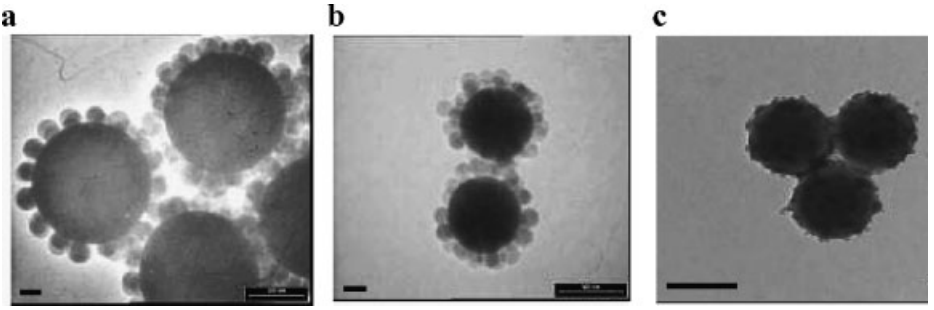

Figure 3.
TEM images of silica/polystyrene composite particles based on 1000 nm (a), 530 nm (b) and 13 nm (c) silica particles. (a, b) polymerization performed using NP_{30} as surfactant and (c) soap-free polymerization. $[SiO_2] = 10$ $g \cdot L^{-1}$ (a, b) and 20 $g \cdot L^{-1}$ (c). Scale bar = 200 nm.

the silica beads can be identified by their size and their contrast. While the largest silica spheres (in dark, Figures 3a and 3b) appear to be regularly surrounded by polystyrene nodules (in grey) forming raspberry-like colloids, the very small silica particles appear to be mainly situated at the surface of the copolymer latex spheres (Figure 3c) although it is hard to conclude from this TEM image whether or not there are also some embedded silica particles. Moreover, it is noteworthy to mention that there is no free silica particles nor free latex spheres in this system which suggests a strong affinity of the growing polymer for the silica particles which are present in large amounts.

The mechanism of composite particles formation can be explained as follows. During the early steps of the polymerization, free molecules of monomer and PEG-MA react to form copolymers. These copolymers will continue to grow until they reach a critical size and become nuclei. Due to the presence of ethylene oxide groups in the structure of the macromonomer, and also because of the presence of the surfactant, these nuclei can become steady and evolve as mature polymer particles.[35] This scenario also holds for the macromonomer adsorbed on the silica surface. In that case, the growing copolymers are expected to strongly attach on silica via the anchored PEG derivative. Free PEG molecules are also initially present in the suspension medium but it can be anticipated that the particles or at least the copolymers they form with styrene will also have a strong tendency to adsorb on silica. In summary, we can briefly describe our system as a self-stabilized copolymerization between the PEG macromonomer and styrene. When very small silica particles are involved in the process, the polymerization is expected to proceed in a similar way except that the primary particles, made of individual silica nanoparticles and polymer chains adsorbed on their surface by means of the macromonomer molecules, coagulate to decrease the overall surface area and become stable mature particles. Due to the hydrophilicity of silica, the later are thrown out of the particle during nucleation and accumulate on the surface of the colloid which situation is presumably the most favorable one from a thermodynamic point of view. If the silica particles really participate to nucleation, we should have an influence of the silica concentration on particles size and polymerization kinetics. Figure 4 shows the evolution of the conversion versus time and of particles size for a series of soap-free polymerizations performed in the presence of silica particles with concentrations comprised between 10 and 80 $g \cdot L^{-1}$.

As predicted, the data in Figure 4 show that the higher the amount of silica, the lower the particles size and the higher the polymerization rate. However, it seems that a minimum silica concentration is required to efficiently stabilize the composite latexes as the polymerization performed with only

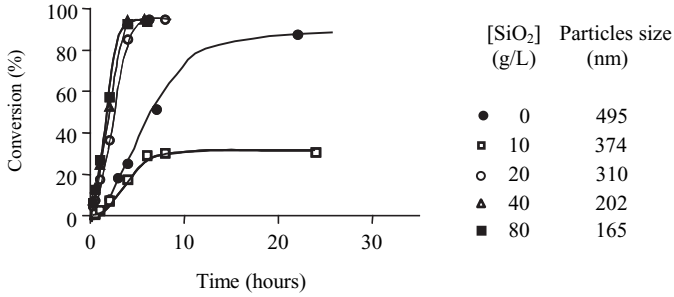

Figure 4.
Conversion versus time curves for a series of soap-free emulsion polymerizations of styrene performed in the presence of macromonomer (2.5 wt% respect to silica) and nanometer sized silica particles. [KPS] = 1 g · L^{-1}. [MMA] = 40 g · L^{-1}. [Styrene] = 160 g · L^{-1}.

10 g/L of silica led to relatively large particles and low conversions.

Laponite/Polymer Composite Particles

Clay Structure

Laponite RD is a fully synthetic clay similar in structure and composition to natural hectorite of the smectite group (Scheme 1). Each layer is composed of three sheets: two outer tetrahedral silica sheets and a central octahedral magnesia sheet. Isomorphous substitution of magnesium with lithium in the central sheet creates a net negative charge compensated by intralayer sodium ions located between adjacent layers in a stack. The cation exchange capacity of Laponite is 0.75 meq · g^{-1}.[36] The dimensions of the elementary platelets are the following: diameter 30 nm and thickness 0.9 nm. In the dry state or in organic solvents, the platelets are piled up into tactoïds of around 2–3 layers thick held together by long-range attractive forces. Reactive silanols, corresponding to structural defects, are located at the broken edges of these stacks while Mg-OH groups are contained into the internal space of the individual clay sheets. Figure 5a is a cryo–TEM image of a suspension of raw Laponite platelets. As mentioned in a previous work,[28] only the crystallites with their basal plane parallel to the observation direction can be clearly seen as dark ''filaments'', as they exhibit a strong diffraction contrast in this orientation. Platelets in other orientations, showing poor absorption contrast, are difficult to detect.

Grafting of the MPS and MPDES Molecules

Grafting of the functional alkoxysilanes was performed in toluene by adding

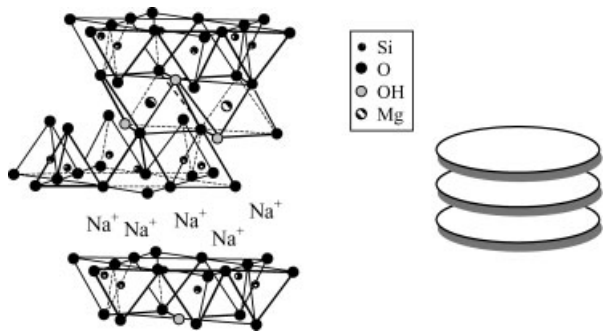

Scheme 1.
Laponite clay structure.

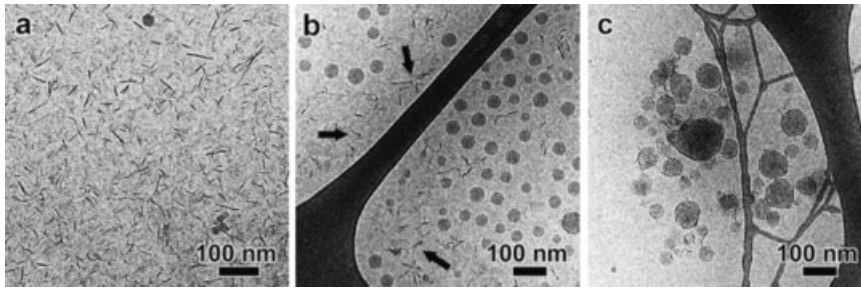

Figure 5.
Cryo-TEM images of: a) a suspension of Laponite platelets (the dark filaments are clay particles seen edge-on); b,c) "hybrid latexes" synthesized by seeded emulsion polymerization of styrene and butyl acrylate in the presence of raw Laponite (b) and 10 wt% of MPDES-functionalized Laponite clay platelets (c). In b, the arrows indicate the presence of Laponite aggregates.

increasing amounts of the coupling agents to the clay suspension. The grafting was qualitatively evidenced by FTIR, ^{29}Si and ^{13}C solid state NMR while the grafted amount was determined by carbon elemental analysis. FTIR indicates successful reaction of the organosilane molecules with the clay edges ($\nu_{C=O}$, 1700 cm^{-1}; ν_{CH}, 2850, 2920 and 2980 cm^{-1} and δ_{CH}, 1380 cm^{-1}). More in depth examination of the carbonyl region showed that both the MPS and the MPDES coupling agents formed hydrogen bonds with the clay surface as the signal of the carbonyl group, which can be detected at 1720 cm^{-1} in the original grafted molecules, was shifted to a lower wavenumber. However, in case of the trialkoysilane MPS coupling agent, a shoulder at 1720 cm^{-1}, which can be assigned to free carbonyl groups, appeared for high grafting densities suggesting the formation of a multilayer coverage. Indeed, MPS molecules can undergo self-condensation in the presence of water giving rise to the formation of polysiloxane oligomers that are attached to the clay edges. These oligomers can also link together the individual platelets and neighbouring clay stacks.

Contrary to the trialkoxysilane, the MPDES coupling agent, cannot condense in solution and forms a monolayer coverage lying flat on the border of the clay plates. Synthesis of the nanocomposite latexes in the presence of grafted Laponite was carried out using 1 g of the organically-modified Laponite suspended into 100 g of water in the presence of SDS and of a peptizing agent. Commercially, peptizers are added to raw Laponite powders in order to retard clay aggregation when the latter is suspended in water (giving rise to the so-called "sol grade"). These molecules are generally multivalent ion salts that bind specifically to the edges of the Laponite platelets. In the case of tetrasodium pyrophosphate ($Na_4P_2O_7$), which was the peptizer used in our study, this tetravalent negatively charged ion adsorbs onto the positively charged rims and thereby effectively screens the rim charge. Under such conditions, satisfactory clay suspensions were obtained in case of the MPDES-grafted Laponite whereas we did not succeed in redispersing the MPS-grafted clay. We presume that this is due to the fact that the clay platelets are irreversibly locked together by siloxane bridges bonding the clay edges as mentioned above. Therefore, in the following, only clay particles modified with the MPDES coupling agent will be involved in the polymerization reaction. Figure 5c shows a cryo-TEM image of c.a. 120 nm copolymer/Laponite nanocomposite particles obtained using MPDES-grafted Laponite as the seed while the micrograph in Figure 5b corresponds to a sample prepared by emulsion polymerization in the presence of raw Laponite. The polymer particles appear as gray spheres and some Laponite crystallites are seen as dark filaments. As

expected, no particular interaction was observed between the clay platelets and the latex particles in Figure 5b. Moreover, some clay aggregates can be clearly seen in between the latex spheres. In contrast, when the monofunctional silane molecule was used as coupling agent, a nanocomposite structure was obtained, the clay platelets constituting a ''shell'' around the polymer latex particles (Figure 5c). Moreover, it is worth noticing that the particles are slightly polygonal as the natural rigidity of Laponite crystals generates a faceting of the surface. It must be underlined that noticeable differences in colloidal stability were observed when bare Laponite was introduced in the polymerization reaction. Although the latexes were stable just after polymerization, they showed only a limited stability with time and coagulation was systematically observed upon storage. This is presumably related to the fact that as the clay platelets were not incorporated within the latex particles, they could form a gel in a similar way as they do in pure water solutions, a mechanism which is additionally promoted by the high ionic strength of the suspension medium. In contrast, successful incorporation of the clay sheets within the polymer particles allowed to achieve a better long term stability of the suspension medium as there were no ''free'' clay plates present in the surrounding aqueous solution.

Adsorption of a Polyethylene Glycol Based Macromonomer

As before for silica, the PEG macromonomer was introduced in the clay suspension to promote *in situ* interactions of the growing radicals with the inorganic surface and generate composite latexes. The interaction of clays with PEO is well known and has been extensively studied in the past.[37–39] Polyethylene oxide polymers have been shown to interact with clay surfaces through ion-dipole interactions between ethylene oxide units and clay ions.[40] Qualitative evidence of the presence of the macromonomer on the clay surface was provided by FTIR spectroscopy after clay separation by precipitation in methanol. Based on our experience on silica, a series of soap-free emulsion polymerization reactions was carried out in the presence of the macromonomer and various concentrations of Laponite in order to establish whether the so-formed clay/macromonomer complexes were able to stabilize the growing latex spheres and influence consequently the polymerization rates and average particle diameters. As expected, polymerizations performed in the presence of the macromonomer but without Laponite gave rise to the formation of big latex spheres (Table 2) and slow polymerization kinetics (Figure 6). In contrast, polymerizations performed in the presence of both the macromonomer and Laponite gave rise to much smaller particles and higher polymerization rates (Figure 6). In addition, the higher the Laponite concentration, the faster was the polymerization reaction as could be expected with regards to the concomittant decrease in particles size with increasing the Laponite concentration (Table 2).

As before for silica, the kinetic data thus suggest that the clay platelets are capable to

Table 2.
Recipe, monomer conversion, particles size and particles number for a series of soap-free emulsion polymerizations of styrene in the presence of macromonomer and increasing concentrations of Laponite.

Runs	Laponite (g/L)	PEG-MA (g/L)	$Na_4P_2O_7$ (g/L)	Conversion[a] (%)	*Dp* (nm)	*Np/L*
1	0	1	2	17	456	$6.8\ 10^{14}$
2	20	1	2	88	205	$3.9\ 10^{16}$
3	30	1.5	3	96	199	$4.7\ 10^{16}$
4	40	2	4	98	167	$8.0\ 10^{16}$
5	60	3	6	99	167	$8.1\ 10^{16}$

[Styrene] = 200 $g \cdot L^{-1}$, ACPA = 0.5 wt% relative to styrene, 70 °C, batch.
[a] Reaction time = 5 hours.

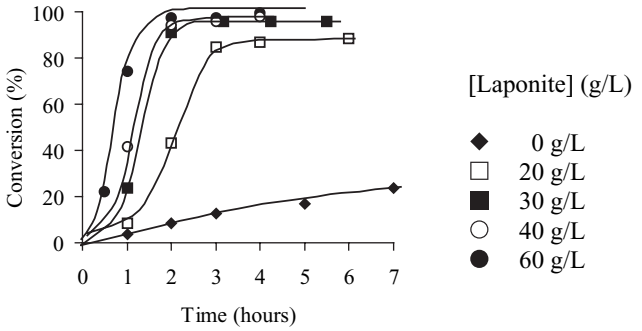

Figure 6.
Conversion versus time curves for a series of soap-free emulsion polymerizations of styrene performed in the presence of the macromonomer but without Laponite (◆) and polymerizations performed in the presence of the macromonomer and increasing Laponite concentrations (□, ■, ○, ●).

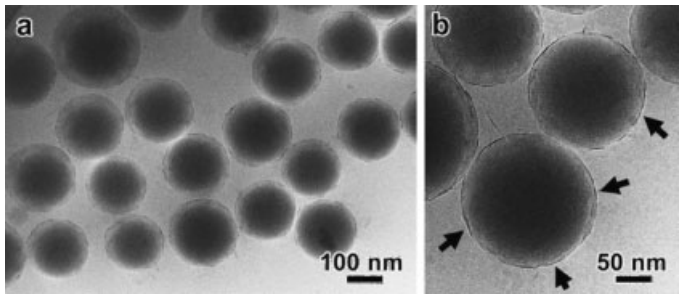

Figure 7.
Cryo-TEM images of spherical polystyrene latex particles stabilized by 10 wt% Laponite crystallites (run 2 in Table 2). In b, the arrows point to a few Laponite platelets seen edge-on on the surface of the polystyrene particle.

stabilize the polymer spheres by accumulating on their surface. To confirm this hypothesis, we analyzed the particles morphology. Figure 7 shows the cryo-TEM image of polystyrene/Laponite composite particles prepared using 10 wt% of the PEG-MA-Laponite complex (run 2 in Table 2). Regular spherical particles with a diameter of around 200 nm are observed. As seen from the distribution of dark ''filaments'' which correspond to the Laponite platelets (see Figure 7a), they are surrounded by clay particles which form a protecting, negatively charged shell structure around the polymer core. The ability of layered silicates to stabilize emulsions or miniemulsions has been reported in several articles.[41–43] The present work gives further evidence that synthetic clay platelets as Laponite can also be used to provide pickering stabilization to polymer latexes produced by emulsion polymerization.

Conclusion

Nanocomposite latexes based on silica and Laponite clay platelets were synthesized through emulsion polymerization using two different strategies which both aimed at to overcome the intrinsic hydrophilic character of the inorganic colloids and promote the growth of polymer on their surface. The mineral particles were modified either by grafting a polymerizable organoalkoxysilane or by the adsorption of a PEG-based macromonomer carrying a terminal MMA group. As far as silica is concerned, we have shown that the morphology of the nanocomposite colloids can be finely tuned by

varying the surface density of the reactive double bonds. Either multipod-like or core-shell morphologies were obtained depending on the silane grafting density. All the results reported in this article support the idea that the nucleation takes place through the capture of the growing radicals by the silica particles. As the latter carry negative charges on their surface, they are able to stabilize the growing latex spheres which number is much larger than in the absence of silica. As the rate in emulsion polymerization is proportional to the particle number, the kinetics of polymerization was strongly accelerated under these conditions. In the second route, double bonds on the silica surface are provided by the adsorption of the PEG macromonomer derivative. The growing polymer nodules are only physisorbed on the mineral surface and homogeneously distributed around the particles forming raspberry-like colloids. The morphology also depends on the silica particle diameter and evolves from raspberry to currant bun with decreasing the silica particles size. In the situation where the polymerization is performed in the presence of very small silica particles and without surfactant, the conversion versus time curves have show that the silica particles participate to the stabilization of the polymer latex spheres giving rise to smaller particles and thus to higher polymerization rates.

In the second part of this article, polymer latexes surrounded by anisotropic Laponite platelets have been successfully obtained by the two routes. It was demonstrated that the clay particles play the role of a pickering stabilizer and are capable to stabilize the composite particles whose diameter depends on the amount of Laponite initially introduced into the reactor. The higher the clay concentration, the larger the composite particle number and, therefore, the higher the polymerization rate as predicted from the emulsion polymerization theory.

Acknowledgements: The authors thank Christian Novat and Nicolas Tissier (LCPP, Villeurbanne) for their great help in TEM analysis. The gift of a sample of Laponite RD by Rockwood Additives is greatly acknowledged.

[1] C. H. M. Hofman-Caris, *New J. Chem.* **1994**, *18*, 1087.
[2] A. D. Pomogalio, *Russ. Chem. Rev.* **2000**, *69*, 53.
[3] G. Kickelbick, *Prog. Polym. Sci.* **2002**, *28*, 83.
[4] V. Castelvetro, C. De Vita, *Adv. Coll. Interf. Sci.* **2004**, *108-109*, 167.
[5] E. Bourgeat-Lami, in "*Encyclopedia of Nanoscience and Nanotechnology*", H. S. Nalwa, Ed., American Scientific Publishers, Los Angeles, **2004**, Vol. 8, pp. 305–332.
[6] E. Bourgeat-Lami, *J. Nanosci. Nanotechnol.* **2002**, *2*, 1.
[7] M. Abboud, L. Casaubieilh, F. Morvan, M. Fontanille, E. Duguet, *J. Biomed. Mater. Res. (Appl. Biomater.)* **2000**, *53*, 728.
[8] E. Bourgeat-Lami, J. Lang, *J. Colloid Interf. Sci.* **1999**, *210*, 281.
[9] S. Chalaye, E. Bourgeat-Lami, J. L. Putaux, J. Lang. *Macromol. Symp.* **2001**, *169*, 89.
[10] D. Hoffmann, K. Landfester, M. Antonietti, *Magnetohydrodyn.* **2001**, *37*, 221.
[11] B. Erdem, D. Sudol, V. L. Dimonie and M. El-Aasser, *J. Polym. Sci., Part A: Polym. Chem.* **2000**, *38*, 4441.
[12] F. Tiarks, K. Lanfester, M. Antonietti, *Langmuir* **2001**, *17*, 5775.
[13] Th. Batzilla, A. Tulke, *J. Coat. Technol.* **1998**, *70*, 77.
[14] C. Barthet, A. J. Hickey, D. B. Cairns, S. P. Armes, *Adv. Mater.* **1999**, *11*, 408.
[15] M. J. Percy, C. Barthet, J. C. Lobb, M. A. Khan, S. F. Lascelles, M. Vamvakaki, S. P. Armes, *Langmuir* **2000**, *16*, 6913–6920.
[16] M. J. Percy, S. P. Armes, *Langmuir* **2002**, *18*, 4562.
[17] M. J. Percy, J. I. Amalvy, D. P. Randall, S. P. Armes, S. J. Greaves, J. F. Watts, *Langmuir* **2004**, *20*, 2184.
[18] J. L. Luna-Xavier, A. Guyot, E. Bourgeat-Lami, *J. Colloid Interf. Sci.* **2001**, *250*, 82.
[19] J. L. Luna-Xavier, A. Guyot, E. Bourgeat-Lami, *Polym. Int.* **2004**, *53*, 609.
[20] J. Zhang, N. Coombs, E. Kumacheva, *J. Am. Chem. Soc.* **2002**, *124*, 14512.
[21] S. Reculusa, C. Poncet-Legrand, S. Ravaine, C. Mingotaud, E. Duguet, E. Bourgeat-Lami, *Chem. Mater.* **2002**, *14*, 2354.
[22] S. Reculusa, C. Mingotaud, E. Bourgeat-Lami, E. Duguet, S. Ravaine, *Nano Letters* **2004**, *4*, 1677.
[23] E. Bourgeat-Lami, M. Insulaire, S. Reculusa, A. Perro, S. Ravaine, E. Duguet, *J. Nanosci. Nanotechnol.* **2006**, *6*, 432.
[24] K. Zhang, H. Chen, X. Chen, Z. Chen, Z. Cui, B. Yang, *Macromol. Mater. Eng.* **2003**, *288*, 380.
[25] N. Negrete-Herrera, J.-M. Letoffe, J.-L. Putaux, L. David, E. Bourgeat-Lami, *Langmuir* **2004**, *20*(5), 564.
[26] N. Negrete-Herrera, S. Persoz, J-L. Putaux, L. David, E. Bourgeat-Lami, *J. Nanosci. Nanotechnol.* **2006**, *6*, 421.

[27] M. Schappacher, A. Deffieux, J.-L. Putaux, P. Viville, R. Lazzaroni. *Macromol.* **2003**, *36(15), 5776.*
[28] N. Negrete-Herrera, J.-M. Letoffe, J.-P. Reymond, E. Bourgeat-Lami, *J. Mater. Chem.* **2005**, *15*, 863.
[29] M. Schappacher, A. Deffieux, J.-L. Putaux, P. Viville, R. Lazzaroni. *Macromolecules* **2003**, *36*(15), 5776
[30] V. Durrieu, A. Gandini, M. N. Belcacem, A. Blayo, G. Eiselé, J.-L. Putaux. *J. Appl. Polym. Sci.* **2004**, *94*(2), 700.
[31] E. Bourgeat-Lami, P. Espiard, A. Guyot, *Polymer* **1995**, *36*, 4385.
[32] D. N. Furlong, J. R. Aston, *Colloids Surf.* **1982**, *4*, 121.
[33] W. Stöber, A. Fink, E. Bohn, *J. Colloid Interf. Sci.* **1968**, *26*, 62.
[34] S. Kang, S. I. Hong, C. R. Choe, M. Park, S. Rim, J. Kim, *Polymer* **2001**, *42*, 879.
[35] R. H. Ottewill, R. Satgurunathan, *Colloid Polym. Sci.* **1995**, *273*, 379.
[36] See for instance: [36a] M. Morvan, D. Espinat, J. Lambard, T. Zemb, *Colloids Surf. Pt. A* **1994**, *82*, 193; [36b] B. S. Neumann, K. G. Sanson, *Israel J. Chem.* **1970**, *8*, 315; [36c] J. D. F. Ramsay, S. W. Swanton, J. Bunce, *J. Chem. Soc. Faraday Trans.* **1990**, *86*, 3919.
[37] R. A. Vaia, S. Vasudevan, X. Krawiec, L. G. Scanlon, E. P. Giannelis, *Adv. Mater.* **1995**, *7*, 154.
[38] P. Arranda, Y. Mosqueda, E. Perez-Cappe, E. Ruiz-Hitzky, *J. Polym. Sci. B: Polym. Phys.* **2003**, *41*, 3249.
[39] E. Loizou, P. Butler, L. Porcar, G. Schmidt, *Macromol.* **2006**, *39*, 1614.
[40] Z. Shen, G. P. Simon, Y. Cheng, *Polymer* **2002**, *43*, 4251.
[41] N. P. Ashby, B. P. Binks, *Phys. Chem. Chem. Phys.* **2000**, *2*, 5640.
[42] S. Cauvin, P. J. Cauvin, S. A. F. Bon, *Macromol.* **2005**, *38*, 7887.
[43] D. K. Voorn, W. Ming, A. M. van Herk, *Macromol.* **2006**, *39*, 2137.

